HIGH CURRENT BEAM SCANNER*

H.E. Wegner and I.L. Feigenbaum
Brookhaven National Laboratory
Upton, New York

The trend in performance of modern accelerators is in the direction of higher beam currents of accelerated ions. Such beams are difficult to handle because of the extreme power densities involved. The maximum utilization of such accelerators is accomplished with elaborate beam transport systems and many experimental stations. However, such systems necessitate an accurate knowledge of both beam shape and position at various critical points. Conventional methods for determining beam position and shape, such as quartz plates or wire-type scanners, fail at high-power densities. In order to observe the beam intensity at the target position while simultaneously studying its shape and position at other locations, a low duty-cycle high-speed scanning system is most desirable because it does not appreciably change the intensity or character of the beam at the target. The speed of the scanner should be sufficient to allow dynamic observation of the tuning conditions of the various beam transport elements, such as quadrupoles and steering magnets, and its corresponding display device should be relatively free of flicker so that eye fatigue is minimized.

A commercially available oscillating-type scanner,[1] designed for scanning the focal plane of mass separators with a fine wire has been modified to meet all of the previous requirements. Modifications included the replacement of the fine wire with a small water-cooled stainless-steel hypodermic tube and the installation of a light source, photodiode, and aperture arrangement that generates fiducial marks on the display corresponding to the X and Y position of the axis of the beam pipe. The water-cooled tube is in the form of a loop arranged so that both X and Y beam profiles are scanned alternately with a single scanner. When the scanner is not in use this loop encircles the beam providing an unobstructed path.

A 1.5 MeV electron beam of 4 mA, focused to a 2 mm spot diameter, and a 4 MeV ion beam of 1 mA focused to a spot size of approximately 3 mm were successfully scanned. The highest beam power density yet scanned corresponded to approximately 35 kW/cm^2 however, heat transport calculations indicate that the scanner should be able to handle beam power densities as high as 80 kW/cm^2 although beam currents corresponding to this power density were not available for testing purposes.

Mechanical Design

The commercial scanner unit[1] consists of a permanently magnetized rotor arranged to be driven by a two pole electromagnet. The rotor is spring-loaded to the neutral position shown in Fig. 1. An oscillating electric signal tuned to the mechanical resonance of the rotor drives the shaft and arm support at a frequency between 10 and 15 Hz depending upon the mechanical load. The single wire provided with the scanner motor is replaced by a continuous piece of 0.64 mm diameter 0.13 mm wall stainless steel tubing looped as shown in Fig. 1 and insulated from the arm. Where the tubing projects from the bottom of the arm it is spiraled several turns to provide flexibility for the oscillation of the shaft. The tubing is soldered into an insulated bushing that penetrates the vacuum wall and terminates in a standard pipe connection. A 100 micron filter is installed in the water inlet to insure against possible plugging of the small diameter tube by dirt particles from the water supply.

As the horizontal and vertical elements of the tubing intercept the axis of the beam pipe, the apertures, as indicated in Fig. 1, expose the photodiode[2] to the light source.[3] The apertures are of different size thus uniquely identifying the X and Y fiducial marks with their respective axes. The large amplitude of oscillation provides a small duty cycle which, when combined with the water cooling of the hollow tube, results in the high beam power-density capability of this design.

The transistorized drive system provided with the drive motor shown in Fig. 1 has a phase-sensitive circuit that senses the voltage induced in the drive coil by the motion of the magnetized armature. The output from the phase-sensitive circuit is electrically related to the absolute position of the rotor. This position information is provided in the form of either a sine or square-wave output. The sine-wave output may be used to trigger the sweep of a standard oscilloscope so that the time axis of the scope effectively becomes coupled to the moving arm at some phase angle. Although the arm moves in sinesoidal fashion, its motion is very nearly linear with time as it crosses the axis because of the large amplitude. Significant nonlinearity can be observed only if the beam is extremely far off axis where the motion of the arm no longer is linear with time. If a linear display is desired under such conditions, the sinesoidal output can be used to drive the horizontal amplifiers of the oscilloscope rather than the time sweep.

Results

A typical beam profile is shown in Fig. 2. The upper trace shows the fiducial marks corresponding to the X and Y axes of the beam pipe. The second trace is the profile of a 250 μA beam

of 3 MeV ions from a Dynamitron accelerator.[4] The trace indicates that the beam is above and slightly to the left of center. The trace also indicates that the beam consists of a sharp central spike superimposed on top of a broad distribution. There is no difficulty with "cross-talk" (ie. secondary electrons scattering from tube to tube) between the horizontal and vertical traces because the profiles are taken at different times rather than simultaneously as is the case with other designs. Careful inspection of the horizontal distribution indicates a slight bulge on the left side that was observed to increase and decrease with a frequency of about one cycle. In the lower traces, the horizontal time sweep was increased by a factor of 4 to show this bulge in more detail. The dotted structure on the peaks is formed by the electronic chopping of the dual-input preamp of the oscilloscope.

With this type of display, the gross pattern showing the X and Y distributions can be moved to the left or right by adjusting the trigger level on the oscilloscope and the separation between the fiducial marks can be adjusted with the time sweep of the oscilloscope. The distance of scan between the two fiducial marks is always 3.5 cm, independent of how the display is adjusted. Hence, if the fine control is adjusted until the fiducial marks are actually 3.5 cm apart on the oscilloscope screen, the observed display bears a one-to-one correspondence with the physical motion of the scanner. The course adjustment factors of two, five, or even ten, may be conveniently used for detailed study of beam shape and position. While it may appear that a more convenient form of display would be to orient the vertical distribution vertically rather than side by side with the horizontal distribution, it takes only a few minutes to become accustomed to the orientation of the two displays; furthermore, the side-by-side comparison has some advantages. For example, if the two profiles are identical, the beam is circularly symmetric; if one is narrower and higher then the beam must be asymmetric. Under actual operating conditions, it appears that the side-by-side display is the more useful. It also is the simplest to obtain with a standard laboratory oscilloscope.[5]

One of the more useful features of this scanner design is that it can be calibrated on the bench without the use of an accelerator beam or any special optical alignment instruments. In practice, the center of the beam port is marked with cross-hairs or a point on the center of a clear window and is illuminated by a stroboscope.[6] The square wave pulse from the scanner drive unit is used to pulse the stroboscope and the output from the stroboscope, indicating the moment of flash, is displayed on the oscilloscope along with the fiducial marks. With this arrangement, the tube is then observed frozen in position and can be viewed over most of its range of oscillation by adjusting the phase control supplied with the scanner drive unit. When the horizontal scanning tube is in coincidence with the center of the beam pipe, the marker pulse from the stroboscope should be in perfect coincidence with the horizontal fiducial mark. The phase control is then adjusted until the vertical scanning portion of the tube is in coincidence with the center axis of the beam pipe and the marker pulse should then be in coincidence with the vertical centering mark. The system can be calibrated in this fashion to 0.2 mm by inspection and can be adjusted by moving the mount slightly until the calibration pulse matches the fiducial marks as desired. This calibration and alignment is then permanent and independent of environmental effects. If the unit is disassembled for any reason, it can easily be recalibrated in a few minutes.

To indicate some of the beam characteristics that can be studied with this scanner, Fig. 3 shows a series of beam profiles under different operating conditions. Trace B shows a 150 μA 2 MeV ion beam from a Dynamitron[7] focused to minimum spot diameter. Trace C shows the same ion beam with horizontal and vertical steering incorporated and it is observed that the various mass components of the ion beam have been separated vertically and horizontally while the neutral component has not been deflected. Traces D and E indicate successive degrees of defocusing with E showing the edges of a three-quarter inch water-cooled collimator that was installed to protect the scanner against missteered beam when not in operation. Trace F shows the best focus condition for a 1100 μA beam corresponding to a beam power density of approximately 4,000 μA/cm^2. In Fig. 3 and all succeeding figures, the relative amplitudes of the various traces are arbitrary and were adjusted to achieve the best comparison. The amplitude does scale to the beam intensity and relative scanner amplitudes may be used to compare beam intensities if desired.

Another series of measurements with a Dynamitron[4] (Fig. 4) shows the shape of the beam with the einsel lens of the ion source adjusted to give a focus beyond the scanner position (Trace B). As the lens is brought up in voltage (Trace C) the focus gradually approaches the position of the scanner until the beam is in focus on the scanner (Trace D). As the lens voltage is further increased, the focus moves forward of the scanner (Trace E) and the shape of the defocused beam is observed to be different on the far side of the crossover (shape at Trace F as compared to Trace B). It is also interesting to note the steering effected by changes in the lens strength; the beam seems to move down and to the left under the best focus conditions.

A second set of measurements is shown in Fig. 5 in which a comparison is made under optimum focus conditions between 1,000 μA beams at 2.0, 3.0, and 3.5 MeV. It is evident that the focal properties get worse at lower energy and the broad defocused portion of the beam increases appreciably from 3.5 MeV (Trace B) to 2 MeV (Trace D). This halo does not appear when the accelerator is used for electron acceleration

when no gas is being introduced into the acceleration tube from the source. Again, the steering effect can easily be observed at the different terminal voltages.

Figure 6 shows a few comparative traces at different current levels for a 1.5 MeV electron beam from a Dynamitron.[8] The beam is focused after leaving the accelerator by a solenoidal lens. In each case the focusing lens has been adjusted to give a minimum spot diameter for that particular current level. It is interesting that the focal properties are best at the highest current level. The multiple traces, B and C, indicate a slight beam instability between successive traverses of the beam scanner. Structural effects observed at lower currents seem to disappear at higher currents. Trace D, taken at the maximum test current of 4,000 μA, indicates that for best focus the beam is elipse-shaped in cross section and not circularly symmetric. Since the electrons fail to stop in the water-cooled tube, they suffer only a dE/dX energy loss in passing through rather than total energy absorption as is the case for comparable energy ion beams. The limit of 4,000 μA was determined not by the scanner but by the available beam stop which had limited power capability. The marker generator was plagued by severe background, as is apparent in Trace A, from electrons scattered to the unshielded diode wiring in the experimental arrangement used for these tests.

Figure 7 shows the type of display observed for a pulsed 1.5 MeV electron beam operating at an instantaneous current level of 10,000 μA. The repetition rate was 3 kc and the pulse length was 10 μ sec. The scanner allowed a direct investigation of the correlation between duty-cycle and focal properties; Traces A and B show optimized and defocused beams for comparison. A time exposure, Trace C, generates an envelope of pulses showing the two profiles. For pulsed operation, a storage oscilloscope would provide a more versatile display since there is a phasing problem between the mechanical frequency of the scanner and the repetition frequency of the accelerator.

Conclusions

It has been shown that a commercially-available scanner can be modified by the addition of an axial marker generator and water-cooled tubes in place of wires so that it can routinely scan high-current accelerator beams up to beam power densities of at least 35 kW/cm^2. The versatility of the scanner has been demonstrated by its use with several different accelerators. In all cases, the installation of the scanner involved only simple adaptation to an existing beam pipe and the device was usually in place and functioning properly in less than an hour's time.

Long term reliability studies have not been made to date, however, the first tube installed failed from apparent radiation damage or sputtering in approximately 20,000 μA hours of all types of test beams. Further measurements with different tube materials will determine which material is best for different kinds of beams and will be reported elsewhere.

Acknowledgments

The test data in this paper could not have been taken without the cooperation of various accelerator groups. We would like to thank Professor A. Taylor for the use of the Cornell 3-MeV Dynamitron, Dr. M.R. Cleland for the use of the Radiation Dynamics Incorporated 4-MeV Dynamitron, and Dr. A. Goland for the use of the Brookhaven National Laboratory 3-MeV Dynamitron.

References

*Work performed under the auspices of the U.S. Atomic Energy Commission.

1. Beam Profile Monitor System, Model 511, manufactured by Danfysik, Jyllinge, Denmark: U.S. Representative-Physicon Co., P.O. Box 232, Boston, Mass. 02114

2. Type 1N2175, manufactured by Texas Instruments Inc., P.O. Box 312, Dallas, Texas

3. Type G.E.-253, manufactured by General Electric Co., Nela Park, Cleveland, Ohio 44112

4. 4 MeV Dynamitron under test at the Radiation Dynamics Co. Inc., Westbury, New York

5. Model 545, manufactured by Tektronix Inc. P.O. Box 500, Beaverton, Oregon 97005

6. Type 1531AB, manufactured by General Radio Co., West Concord, Mass. 01781

7. 3 MeV Dynamitron, Engineering Dept., Cornell University, Ithaca, New York

8. 3 MeV Dynamitron, Dept. of Physics, Brookhaven National Laboratory, Upton, New York

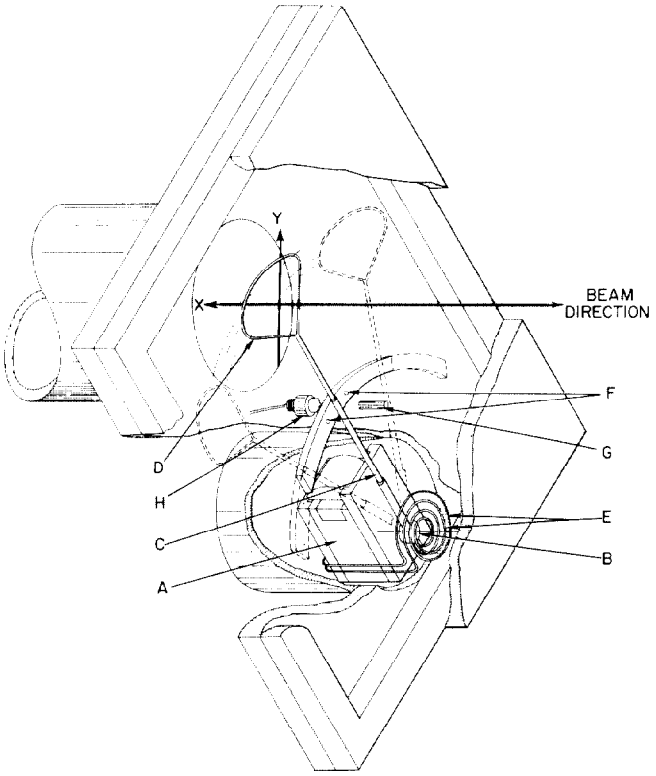

Fig. 1. Beam profile scanner arrangement: The two-pole electromagnet A oscillates the rotor and drive shaft B which oscillates the support arm C and water-cooled tube D. The feed and return lines are spiraled, E, for flexability. As the X and Y axial positions are crossed by the horizontal and vertical elements of the tube loop, apertures F expose the photodiode G to the light source H resulting in the fiducial marks corresponding to the axis of the beam pipe.

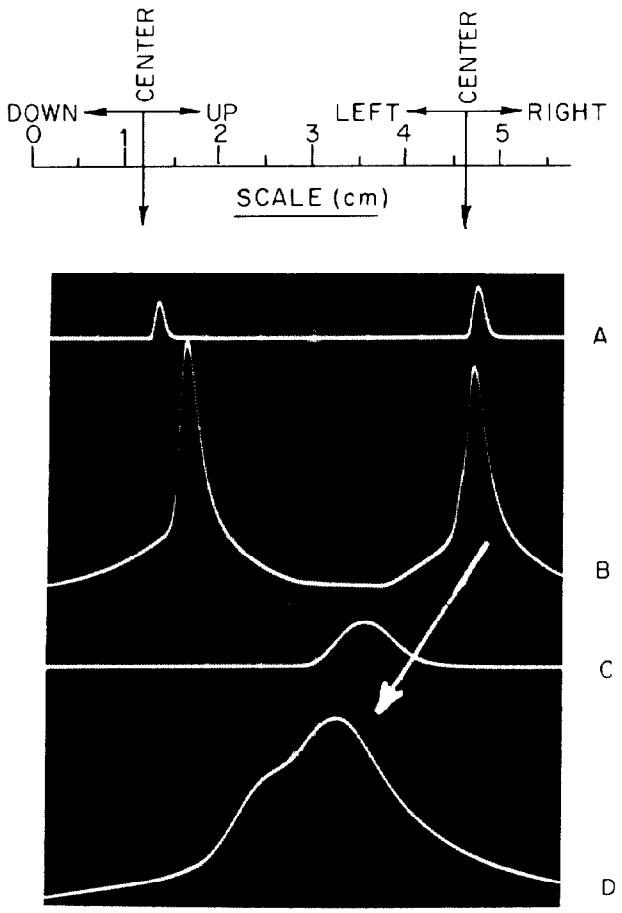

Fig. 2. Typical oscilloscope beam profile display for a 3 MeV hydrogen ion beam of 240 μA. Trace A shows the vertical and horizontal fiducial marks indicating the axis of the beam pipe; Trace B shows the beam profile; Traces C and D are A and B with a 4X increase in sweep speed that shows the structure in more detail.

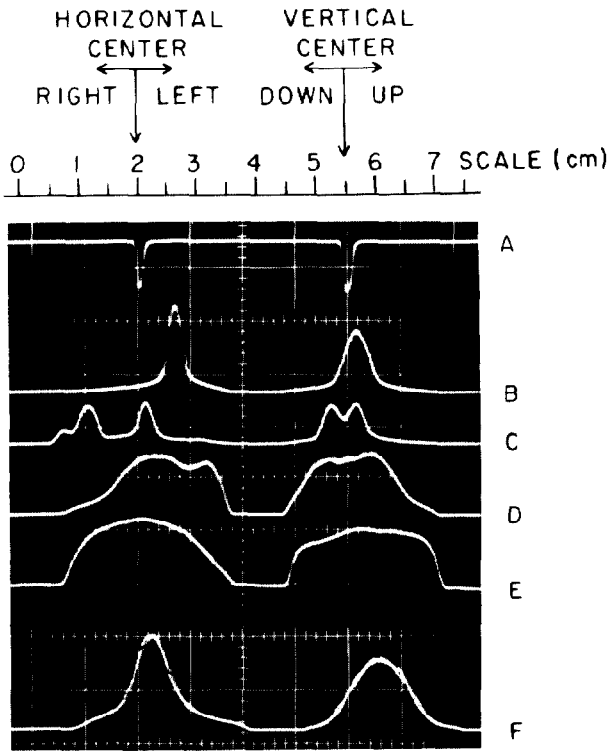

Fig. 3. Comparison of various operating conditions for a 2 MeV hydrogen ion beam. Trace A is the X-Y axis marker-trace; B is the best focus at 180 μA; C is best focus with magnetic steering; D is partially defocused; E is completely defocused; F is the best focus for an 1100 μA hydrogen ion beam.

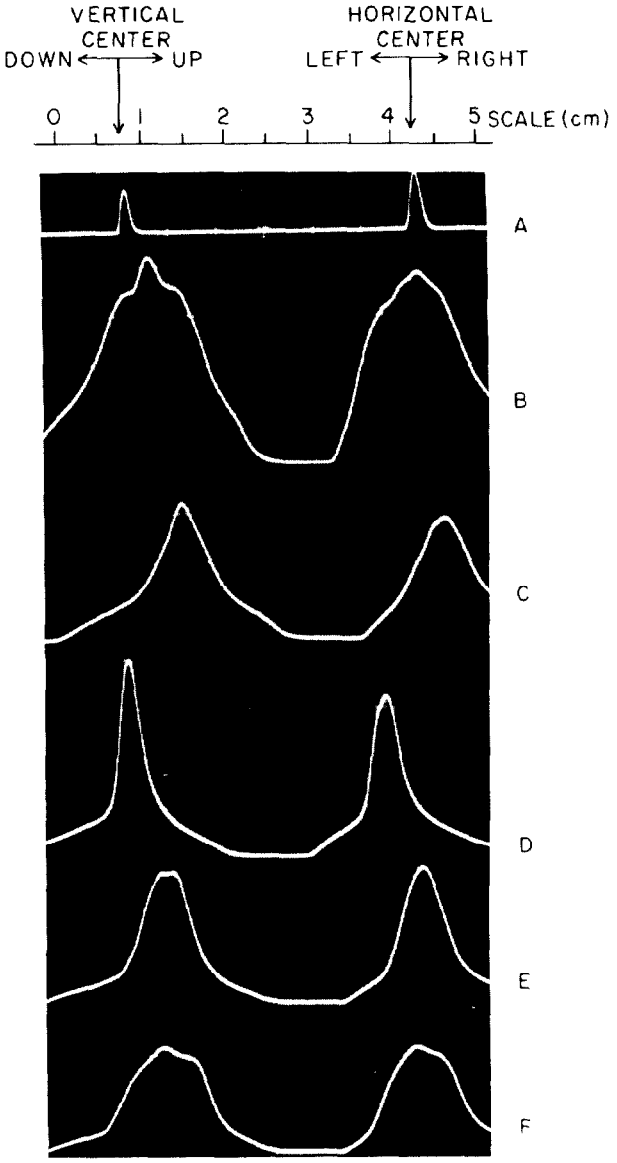

Fig. 4. Comparison of different einzel-lens focal conditions at 3 MeV for a 570 μA hydrogen ion beam. Trace A is the X-Y axis marker trace; Trace B, 14.1 kV; focus beyond scanner; Trace C, 15.0 kV, focus nearer scanner; Trace D, 16.2 kV, focus at scanner; Trace E, 17.4 kV, focus before scanner; Trace F, 18.3 kV, focus further before scanner. Note steering effect at different lens voltages.

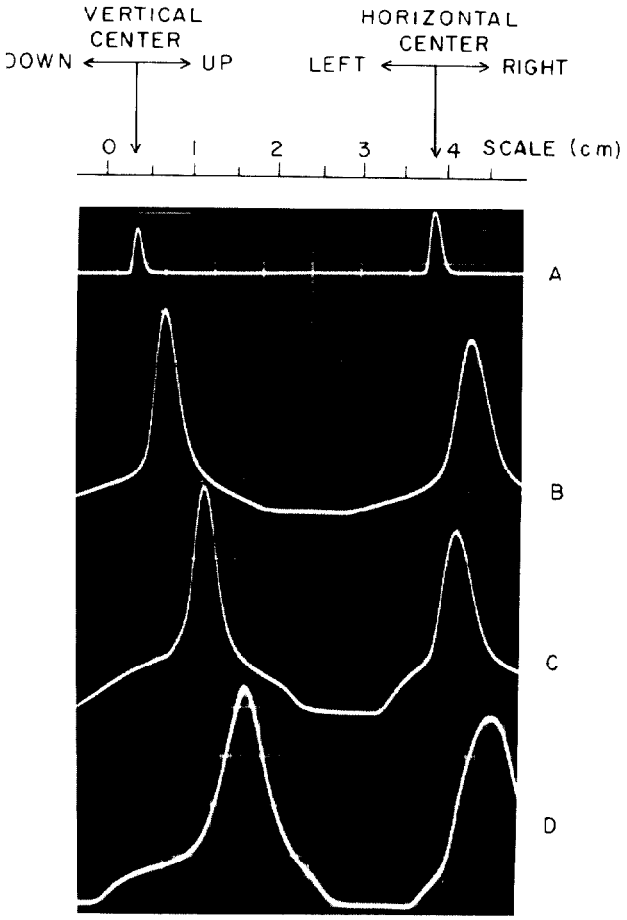

Fig. 5. Comparison of 2.0, 3.0, and 3.5 MeV 1000μA hydrogen ion beams. Trace A is the X-Y axis marker trace; Trace B, 3.5 MeV; Trace C, 3.0 MeV; Trace D, 2.0 MeV. Note steering effect at different energies.

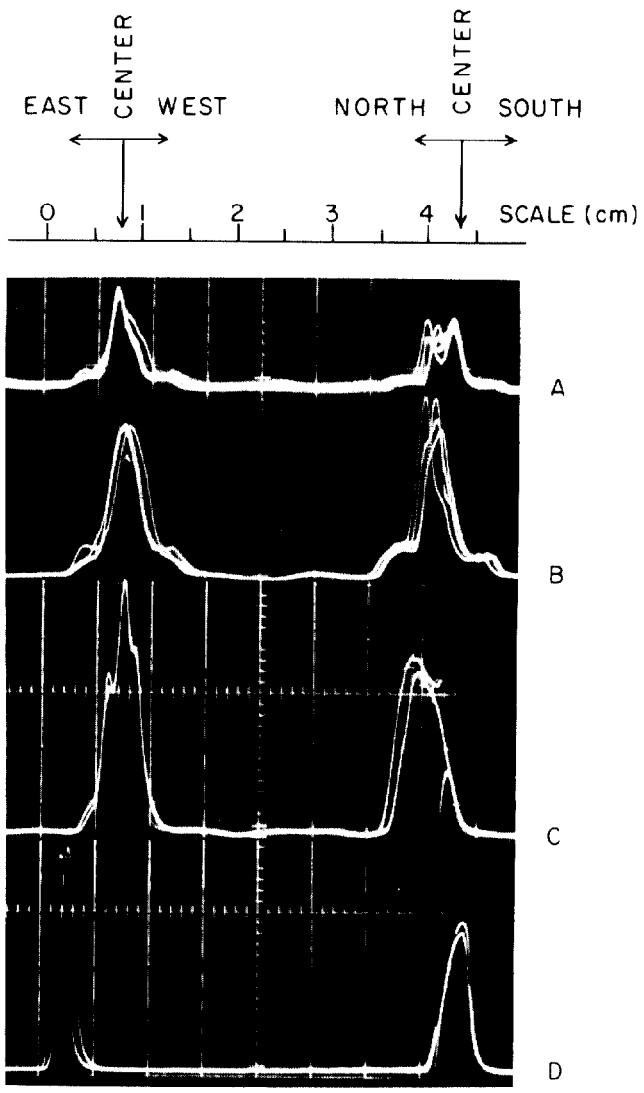

Fig. 6. Comparison of 1.5 MeV electron D.C. beams. Trace A is the X-Y axis marker trace and shows scattered electron pickup from Trace B corresponding to 200μA; Trace C, 1,000μA; Trace D, 4000μA.

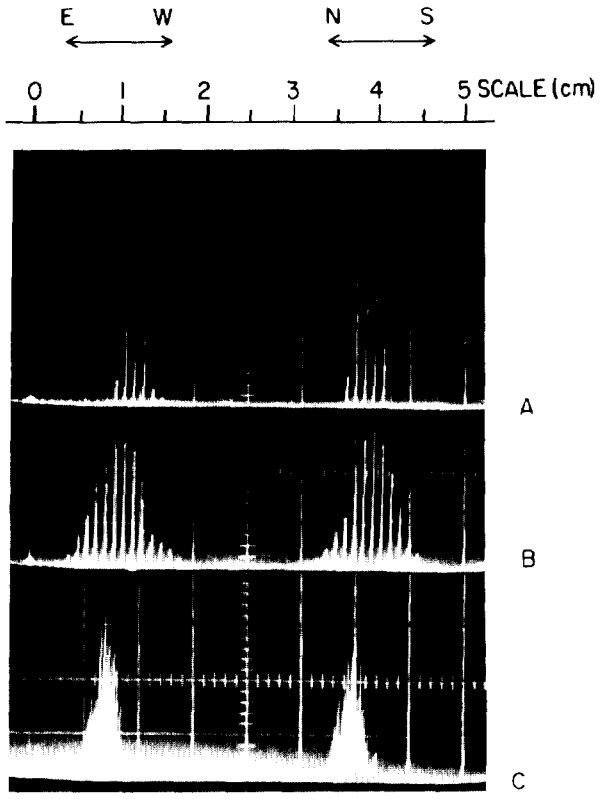

Fig. 7. Comparison of different focal conditions for 1.5 MeV pulsed electron beam; 3 kHz, 10 μ s, 10,000 μ A average current; Trace A, best focus profile; Trace B, defocused; Trace C, time exposure of best focus.